Supporting Information

Cross-linking of Orai1 channels by STIM proteins

Yandong Zhou, Robert M. Nwokonko, Xiangyu Cai, Natalia A. Loktionova, Raz Abdulqadir, Ping Xin, Barbara A. Niemeyer, Youjun Wang, Mohamed Trebak, and Donald L. Gill

SI Materials and Methods

DNA Constructs. Monomer SOAR1 was inserted into pEYFP-C1 (Clontech) between XhoI/EcoRI sites as previously described (1). To obtain YFP-$SOAR_{2.1}$, the SOAR fragment of YFP-STIM2.1 (from Dr. Barbara Niemeyer, Homburg) was amplified and inserted into pEYFP-C1 between XhoI/EcoRI sites. The concatemeric SOAR1 dimer (YFP-S-S) and mutated (F394H) derivatives (YFP-S-S_H, YFP-S_H-S and YFP-S_H-S_H) were as previously described (1). The new concatemeric SOAR dimers (YFP-$S_{2.1}$-$S_{2.1}$ and YFP-$S_{2.1}$-S) were constructed similarly, using the 72-bp linker 5'-GGCGGCTCTGGAGGTAGCGGAGG TGGAATTCTGCAGTCGAGGGGTGGATCCGGTGGGTC CGGCGGATCCGGC-3' (translated as the 24 amino acids GGSGGSGGGILQSRGGSGGSGGSG) between SOAR units. The intramolecular YFP-STIM1-CFP construct, used to convert the intensity ratio of YFP/CFP to molar ratio, was made by inserting ECFP into the pDS-YFP-STIM1 vector at the AflII/BamHI site using the following primers: FP 5'-TGGGAGGTCTTAAGAAGGCGAGCTCGACTAGTGAAC CG-3'; RP 5'-GAGATCTGGATCCCTACTTGTACAGC-3'. The mCherry-STIM1 plasmid was provided by Dr. Madesh Muniswamy (Temple Univ.). To convert the intensity ratio of mCherry/YFP to molar ratio, we constructed a new calibrator molecule, mCherry-STIM1-YFP. EYFP was inserted at the C-terminus of STIM1 at the AflII/BglII sites using the following primers: FP 5'-TGGGAGGTCT TAAGAAGGCGAGCTCGACTAGTGAACCG-3' and RP 5'-TCGAGATCTGAGTCCCTACTTGTACAGC-3'. Point mutations were generated using the QuikChange Lightning Site-Directed Mutagenesis Kit (Agilent Cat No. 210518). All constructs were confirmed by sequencing before transfection.

Generation of Human STIM1/STIM2 Double Knock-out Cell Lines Using the CRISPR-Cas9 Nickase System. STIM1 or STIM2 sequence-specific guide RNAs were inserted into the LentiCRISPR V2 vector (Addgene #52961) with the BsmB1 restriction site, to create a gRNACas9-encoding plasmid. HEK cells were transfected with the gRNA-Cas9 plasmid using electroporation at 180 V, 25 ms in 4 mm cuvettes (Molecular Bio-Products) using the Bio-Rad Gene Pulser Xcell system in OPTI-MEM medium. 48 hours later, cells were cultured in Dulbecco's modified Eagle's medium (DMEM) supplemented with 10% fetal bovine serum (FBS), penicillin (100 UI), streptomycin (100 µg/ml) and puromycin (2 µg/ml) in 5% CO_2 at 37°C. 5 days later, cells were collected and seeded at 1 cell per well into 96-well plates without puromycin. Disruption of the stim1 and stim2 genes in individual colonies was detected using the Guide-it Mutation Detection Kit (Clontech Laboratories, #631443), and confirmed by sequencing as well as Western Blot and functional responses (Fig. S8). The STIM1/STIM2-double knockout cell line generated was named "HEK-S1S2-dKO". Oligonucleotides used for creating the STIM1/STIM2 guide RNAs were: STIM1 g-RNA F: 5´-TGGTGAGGATAAGCTCATC -3´; STIM1 g-RNA R: 5´-GATGAGCTTATCCTCACCA-3´; STIM2 g-RNA F: 5´-AGATGGTGGAATTGAAGTAG -3´; STIM2 g-RNA R: 5´-CTACTTCAATTCCACCATCT-3´.

Cell Culture and Transfection. All non-transfected HEK cells were cultured in DMEM medium (Mediatech; 10-013-CV)) supplemented with 10% FBS, penicillin and streptomycin (Gemini Bioproducts, CA) at 37°C with 5% CO_2. HEK cells stably expressing Orai1-CFP (HEK Orai1-CFP), or Orai1-His (HEK Orai1-His), or Orai1-HA (HEK Orai1-HA) were cultured in the same medium as above supplemented with G418 (100 µg/ml). HEK-S1S2-dKO cells generated by the CRISPR-Cas 9 system derived as described above were cultured in the same medium without G418. All transfections were undertaken by electroporation at 180 V, 25 ms in 4 mm cuvettes (Molecular Bio-Products) using the Bio-Rad Gene Pulser Xcell system in OPTI-MEM medium. For cell lines transfected with plasmids which resulted in constitutive Ca^{2+} entry (all active monomeric or concatemeric SOAR plasmids), following transfection cells were cultured in growth medium supplemented with 600 µM EGTA to reduce extracellular Ca^{2+}. All experiments commenced 18-24 hours after transfection.

Cytosolic Ca^{2+} Measurements. Cytosolic Ca^{2+} levels were measured by ratiometric imaging using fura-2 between 18-24 h after transfection as described earlier (2). Loading of fura-2 and imaging were performed in Ca^{2+}-free solution containing (mM): 107 NaCl, 7.2 KCl, 1.2 $MgCl_2$, 11.5 glucose, 20 Hepes-NaOH, pH 7.2. 1 mM $CaCl_2$ was added as indicated in experiments. Loading of cells with 2 mM fura-2/AM was for 30 min at room temperature, followed by treatment with fura-2-free solution for a further 30 min. Fluorescence ratio imaging was measured utilizing

the Leica DMI 6000B fluorescence microscope and Hamamatsu camera ORCA-Flash 4 controlled by Slidebook 6.0 software (Intelligent Imaging Innovations; Denver, CO) as previously described (3). Consecutive excitation at 340 nm (F_{340}) and 380 nm (F_{380}) was applied every 2 sec and emission fluorescence was collected at 505 nm. Intracellular Ca^{2+} levels are shown as F_{340}/F_{380} ratios obtained from groups of >15 single cells per coverslip. All Ca^{2+} imaging experiments were performed at room temperature and representative traces of at least three independent repeats are shown as means ± SEM.

Förster Resonance Energy Transfer (FRET) Measurements. Analysis of FRET was undertaken similarly to that described earlier (3). To determine FRET signals between stably expressed Orai1-YFP and transiently expressed YFP-tagged monomer SOAR or concatemeric SOAR, we used the Leica DMI 6000B inverted automated fluorescence microscope equipped with CFP (438Ex/483Em), YFP (500Ex/542Em), and FRET (438Ex/542Em) filter cubes. Images were captured at 20 s intervals to minimize photobleaching. At each time point, 3 sets of images (CFP, YFP and FRET) were collected at room temperature using a 40× oil objective (N.A.1.35; Leica) and processed using Slidebook 6.0 software (Intelligent Imaging Innovations). Images were captured at 20 sec intervals. Exposure times for the CFP, YFP and FRET channels were 1000 ms, 250 ms, and 1000 ms, respectively. The decreased YFP channel exposure time compensates for the greater fluorescence intensity of YFP compared to CFP. Three-channel corrected FRET was calculated using the formula:

$$F_C = I_{DA} - Fd/Dd * I_{DD} - Fa/Da * I_{AA}$$

in which I_{DD}, I_{AA} and I_{DA} represent intensity of the background-subtracted CFP, YFP and FRET images, respectively. F_C represents the corrected energy transfer. Fd/Dd represents measured bleed-through of CFP through the FRET filter (0.457), and Fa/Da is measured bleed-through of YFP through the FRET filter (0.190). We used the E-FRET method to analyze 3-cube FRET images as described by Zal and Gascoigne (4) using the formula:

$$E_{app} = Fc / (F_C + G * I_{DD}).$$

where G is the instrument specific constant. The value of G was determined by measuring the CFP fluorescence increase after YFP acceptor photobleaching using HEK cells transiently transfected with the pEYFP-ECFP construct as described earlier (1). The value of G was calculated to be 1.9 ± 0.1. For all E-FRET summary data, the region of interested was close to the plasma membrane, and cells with similar YFP/CFP ratios were used for E-FRET analysis.

Super-Resolution STED Image Analysis. HEK Orai1-His or HEK Orai1-CFP cells were transfected with YFP-S-S or YFP-S_H-S constructs and imaged 14-20 hr after transfection. The live cell images were collected on the inverted Leica TCS SP8 confocal microscope equipped with STED (STimulated Emission Depletion) using a 63x/1.40 Oil objective. The deconvolution of STED images were undertaken by Huygens Deconvolution software (Scientific Volume Imaging). Images shown are typical of at least three independent experiments.

Fluorescence Recovery After Photobleaching (FRAP) Measurements. FRAP measurements were undertaken on a Leica TCS SP8 confocal microscope with a 40X oil objective at a zoom of 1.5X. The microscope was equipped with a live cell chamber system providing 5% CO_2 and 37°C. To minimize background bleaching of the sample during measurement, YFP was excited with the 488 nm laser at 0.3% output. The pinhole was set at 1.0 Unit and no line averaging was used. Focus was adjusted to the plasma membrane adjacent to the coverslip. The circle tool was used to define the region of interest (ROI) bleach area with a diameter of 3.0 µm (<5% of cell area). For each FRAP measurement, the ROI in a photobleached cell was compared to the same size ROI in an otherwise identical but unbleached reference cell in the same field of view (5). In each case, background fluorescence subtracted. For photobleached cells, YFP bleaching was for 8 sec (488 nm laser, 100% output). Before photobleaching, 6 images were obtained to give the prebleached fluorescence level, then 100 post-bleach images were collected every 3 sec (averaged into 15 sec intervals). The values for fluorescence in the photobleached cell were corrected for the rate of fluorescence decay measured in the reference cell, and expressed as a normalized fluorescence percentage. To calculate the immobile fraction percentage of SOAR-Orai1 complexes and to compare recovery rates, the pre-bleach intensity was normalized to 100%. An exponential one-phase association model was used to fit the recovery phase in order to obtain the half-life, $\tau_{1/2}$ for fluorescence recovery, and the mobile fraction (MF) (5). The diffusion coefficient (D) was calculated by the formula: $D = 0.224r^2/(\tau_{1/2})$, in which r is the bleached circle region radius. The immobile fraction (IF) was obtained as: F=100-MF. Statistics for FRAP shown as means ± SEM.

Electrophysiological measurements. Patch-clamp recordings were performed on HEK Orai1-CFP or HEK Orai1-His cells transiently expressing YFP tagged WT-SOAR1 homodimer or heterodimers containing either one F394H mutant unit or one SOAR2.1 unit. To maintain the ER store-repleted state, the pipette solution contained (in mM): 135 Cs-Aspartate, 10 HEPES, 4 $MgCl_2$, 10 EGTA, and 3.6 $CaCl_2$ (pH 7.2 with CsOH). The amount of EGTA and $CaCl_2$ were calculated using WEBMAXCLITE (http://web.stanford.edu /~cpatton/webmaxc2) so that the cytosolic Ca^{2+} was maintained at ~90 nM throughout experiments. To passively deplete ER stores, the pipette solution contained (in mM): 135 Cs-Aspartate, 10 HEPES, 8 $MgCl_2$, and 10 BAPTA (pH 7.2 with CsOH). The 20 mM Ca^{2+} bath solution contained (in mM): 130 NaCl, 4.5 KCl, 5.0 HEPES, 10 Dextrose, 10 TEA-Cl and 20 $CaCl_2$ (pH 7.4 with NaOH). The Ca^{2+}-free bath solution contained (in mM): 150 NaCl, 4.5 KCl, 5.0 HEPES, 10 Dextrose, 10 TEA-Cl and 3 mM $MgCl_2$ (pH 7.4 with NaOH). Currents were recorded in the standard whole-cell configuration using an EPC-10 amplifier (HEKA). Glass electrodes with a typical resistance of

2-4 MΩ were pulled using a P-97 pipette puller (Sutter Instrument). A 50-ms step to -100 mV from a holding potential of 0 mV, followed by a 50-ms ramp from -100 to 100 mV, was delivered every two seconds. Currents were filtered at 3.0 kHz and sampled at 20 kHz. A +10 mV junction potential compensation was applied to correct the liquid junction potential between the bath and pipette solutions. Currents recorded before Ca^{2+} stores were emptied (for activation of Orai1 with full-length STIM due to store depletion) or in Ca^{2+}-free solution (for constitutive activation conditions with SOAR proteins) were subtracted to obtain leak-free currents. All data was acquired with Patch Master and analyzed using FitMaster and Prism. The rig was equipped with a Leica DMI 3000B manual microscope and Hamamatsu camera ORCA-R^2 controlled by Slidebook 6.0 software (Intelligent Imaging Innovations; Denver, CO). To assure that Orai1 was in excess, it was necessary to determine the molar ratio between Orai1-CFP and YFP tagged SOAR dimers. To do this, we calibrated the relative YFP/CFP fluorescence ratio using a STIM1 "calibration construct" with both N-terminal YFP and C-terminal CFP tags on the same molecule (YFP-STIM1-CFP). This calibration construct was expressed in HEK cells, and the ratio of YFP/CFP fluorescence was measured with stores emptied with ionomycin, to assure maximal YFP-CFP distance and hence minimal FRET between YFP and CFP, as we described previously (1). Intensity of YFP and CFP from the calibration construct were obtained under the same conditions used to obtain images for Orai1-CFP and YFP-SOAR dimers in order to determine actual expression levels used during whole cell patch experiments. As shown in Fig. S4*B-F*, using the YFP-CFP calibration construct with equal YFP and CFP protein, the YFP:CFP fluorescence intensity ratio was 4.204 ± 0.191. In other words, when the ratio of YFP:CFP is equal to 4.204, the number of YFP and CFP molecules is equal. For patch-clamp studies undertaken in HEK Orai1-CFP cells, we only analyzed cells with a YFP/CFP ratio smaller than 4.2 (Fig. S4*G* and *J*) to assure that Orai1-CFP was in excess over YFP-SOAR dimers. We also assured that the non-fluorescently tagged Orai1-His protein was in excess over YFP-SOAR dimers. To do this, we compared the Orai1 protein expression levels in HEK Orai1-His and HEK Orai1-CFP cells by Western analysis. As shown in Fig. S4*A*, Orai1-His expression was higher than Orai1-CFP. Thus, for patch-clamp studies in HEK Orai1-His cells, we analyzed only cells with similar YFP-SOAR dimer expression levels as used in HEK Orai1-CFP cells (Figure S4*H,I,K,* and *L*).

Western Blots. Cells were lysed in pre-chilled lysis buffer containing 150 mM NaCl, 10 mM Tris-HCl (pH 7.4), 1% NP-40, and one tablet of complete protease inhibitors (Santa Cruz, sc-29131) per 25 ml. Lysis took place on ice for 30 min, followed by centrifugation at 14,000 g, 4°C for 10 min. Supernatants were quantified using the Bio-Rad DC protein assay kit. Protein extracts (27µg per lane) were resolved on 4-12% NuPAGE Bis-Tris precast gels (Life Technologies) and transferred to Bio-Rad Immuno-Blot PVDF membranes (162-0177, Bio Rad). After transfer, PVDF membranes were blocked in phosphate-buffered saline-Tween 20 (PBST; containing 1X PBS (46-013-CM, Mediatech), 0.1% Tween 20) containing 5% non-fat dried milk (M0841, LabScientific) for 1 h at room temperature, then incubated overnight at 4°C with one of four different primary antibodies: Orai1 antibody (1:1000; O8264, Sigma); GAPDH antibody (1:1000; MAB374, EMD Millipore Corp); STIM1 antibody (1:1000; 4149S, Cell Signaling); STIM2 antibody (1:1000; 4917S, Cell Signaling). Membranes were washed three times (7 min) in PBST and incubated with secondary antibodies for 30 min at room temp. Subsequently, membranes were washed 3 times (5 min) in PBST. Peroxidase activity was measured with SuperSignal West Pico Chemiluminescent Substrate (Thermo Scientific) following the manufacturer's protocols; the resulting fluorescence was collected using a FluorChem M image system from ProteinSimple. Quantification analysis was performed using Image J.

Structural modeling. As shown in Fig. S7, the structure simulation function of the Chimera software was used to predict the structure of SOAR region of STIM2.1 (Cyan) (6). The solved crystal structure of the SOAR domain from STIM1 (PDB ID: 3TEQ) was selected as the template (7).

Statistics: All the data analyses were performed with GraphPad Prism 7 (GraphPad Software). Where shown in figures, Student's t test was used for statistical comparisons between two groups. Data are presented as means ± SEM.

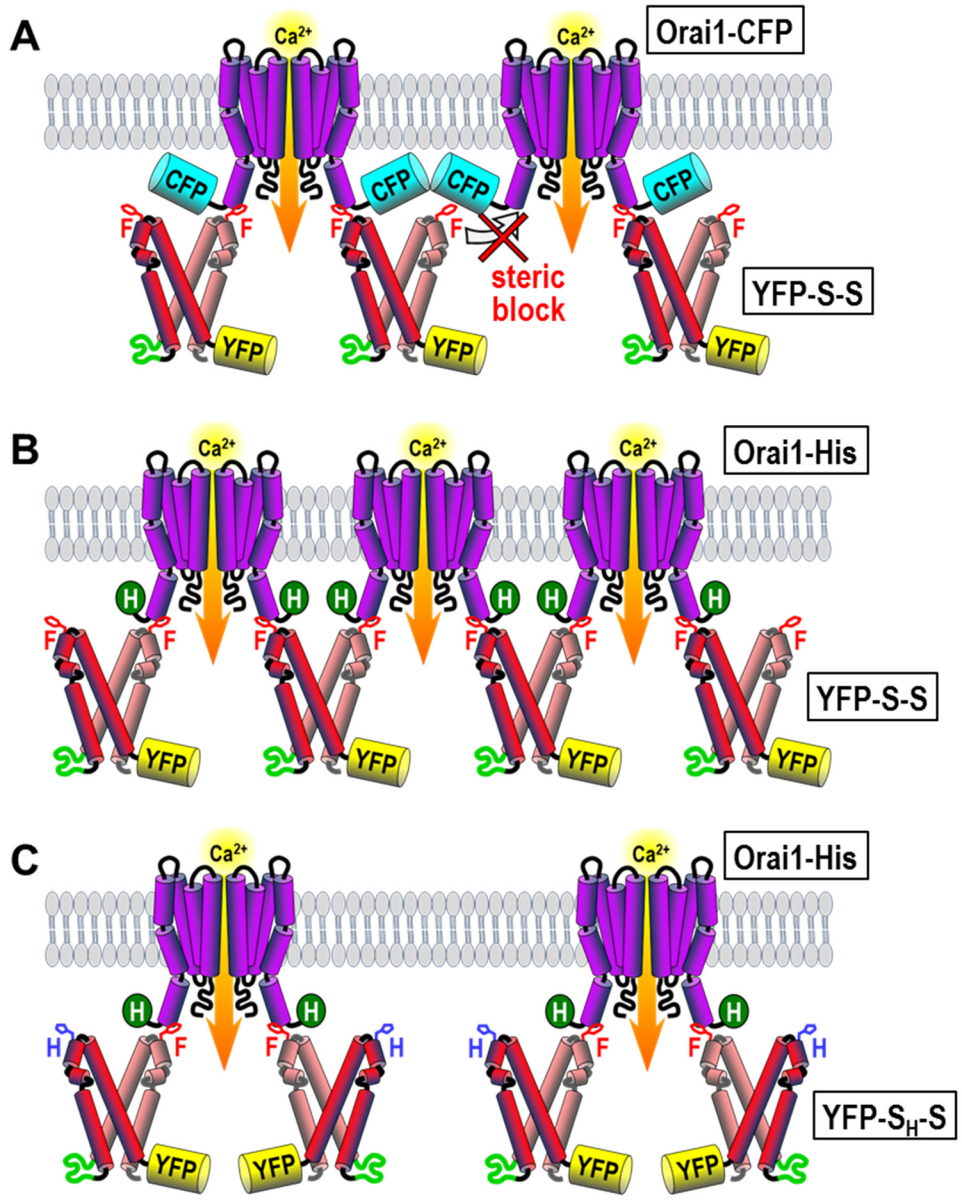

Fig. S1. Schematic model of the interaction between SOAR dimers and Orai1 hexamers in the PM. (*A*) The cross-linking of Orai1-CFP by the YFP-S-S homodimer is prevented by the bulky CFP tag on the Orai1 C terminus as result of steric hindrance. (*B*) Using Orai1-His which has a small (5 amino acid) C terminal tag, YFP-S-S can effectively cross-link two adjacent Orai1 hexamers in the PM. (*C*) Even with Orai1-His, YFP-S_H-S dimers fail to cross-link Orai1 hexamers due to the inability of the F394H mutated SOAR monomer (S_H) to bind to the Orai1 channel. Note that the CFP tag on the Orai1 C-terminus does not affect the interaction of SOAR with the Orai1 channel. The CFP-tag only sterically prevents the SOAR-mediated cross-linking between separate Orai1 channels.

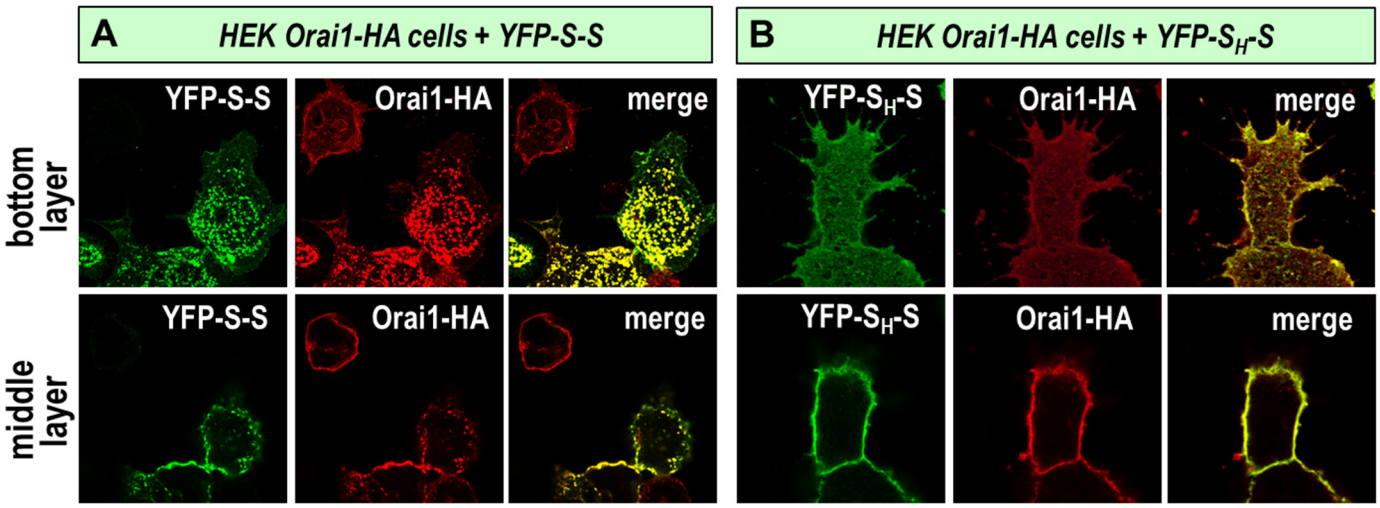

Fig. S2. Confocal images of HEK cells stably expressing Orai1 labeled at the C terminus with the 9 amino acid hemagglutinin tag (Orai1-HA). *(A)* YFP-S-S transiently expressed in HEK Orai1-HA cells, was immunostained with antibodies targeting either to YFP (green, left panels), or Orai1 (red, middle panels), with the merged images in the right panel. Similar levels of Orai1 and SOAR clusters were observed as seen with Orai1-His expressing cells (see Fig. 1*E-F*). While clustering was more pronounced in the bottom cell layer (top panels), we also observed strong clustering along the cell periphery by imaging the middle cell layer (bottom panels). *(B)* Immunostaining reveals that the heterodimer YPF-S_H-S is still unable to cause clustering in cells expressing Orai1-HA. Images are representative of three independent experiments.

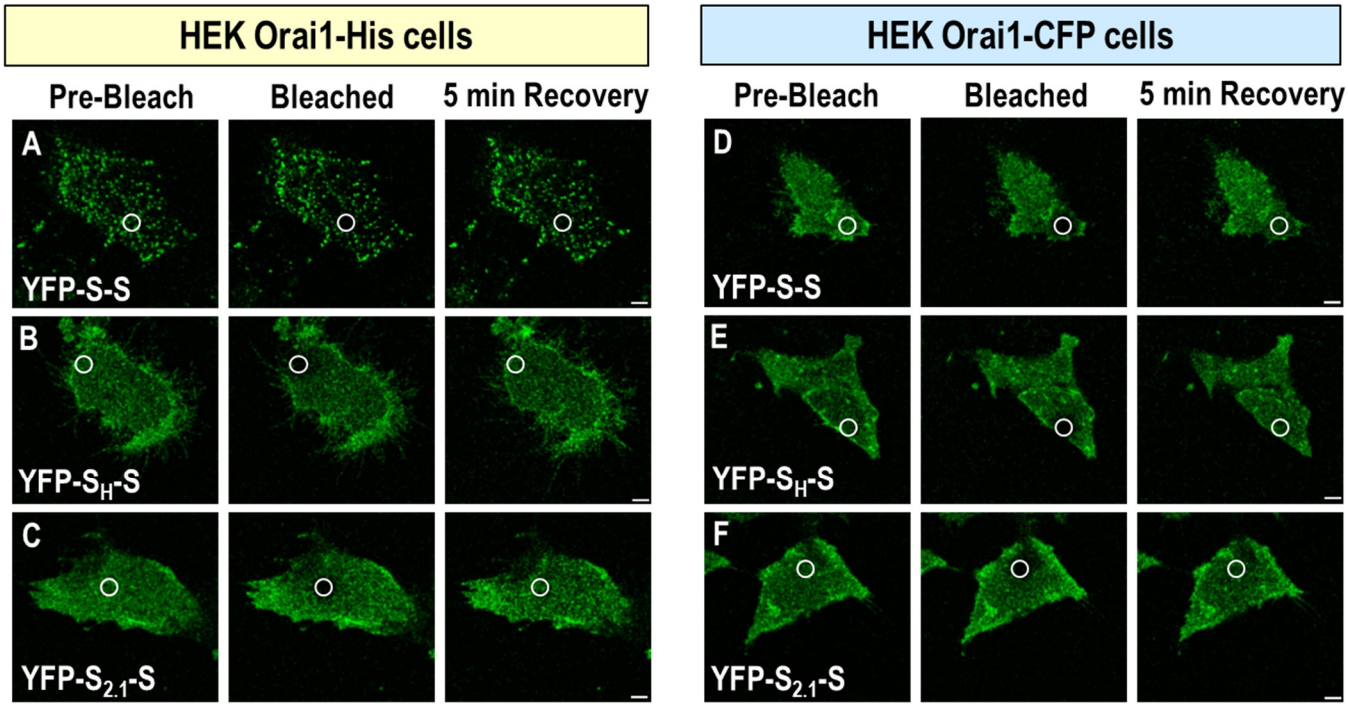

Fig. S3. Fluorescence recovery after photobleaching (FRAP) experiments to measure diffusional parameters of cross-linking by SOAR dimers. Images were focused on the plasma membrane adjacent to the coverslip. Circles represent bleached target areas (approximately 3 μm). *(A-C)* Using HEK Orai1-His cells: clusters were clearly visible in cells co-expressing YFP-S-S *(A)*, whereas cluster formation was not seen in cells co-expressing either YFP-S_H-S *(B)* or YFP-$S_{2.1}$-S *(C)*. The left panels are images taken before bleaching, and fluorescence is clearly visible within the selected regions. The middle panels are images collected immediately after photobleaching for 8 sec. After 5 minutes of recovery, the post-bleach images reveal that much of the fluorescence returns for YFP-S_H-S (*B*) or YFP-$S_{2.1}$-S (*C*), whereas much less returns to the bleached areas for YFP-S-S (*A*). In cells stably expressing Orai1-CFP (*D-F*), we observe no difference in the distribution and recovery of either YFP-S-S *(D)*, YFP-S_H-S *(E)* or YFP-$S_{2.1}$-S (*F*). Representative images are from three independent experiments.

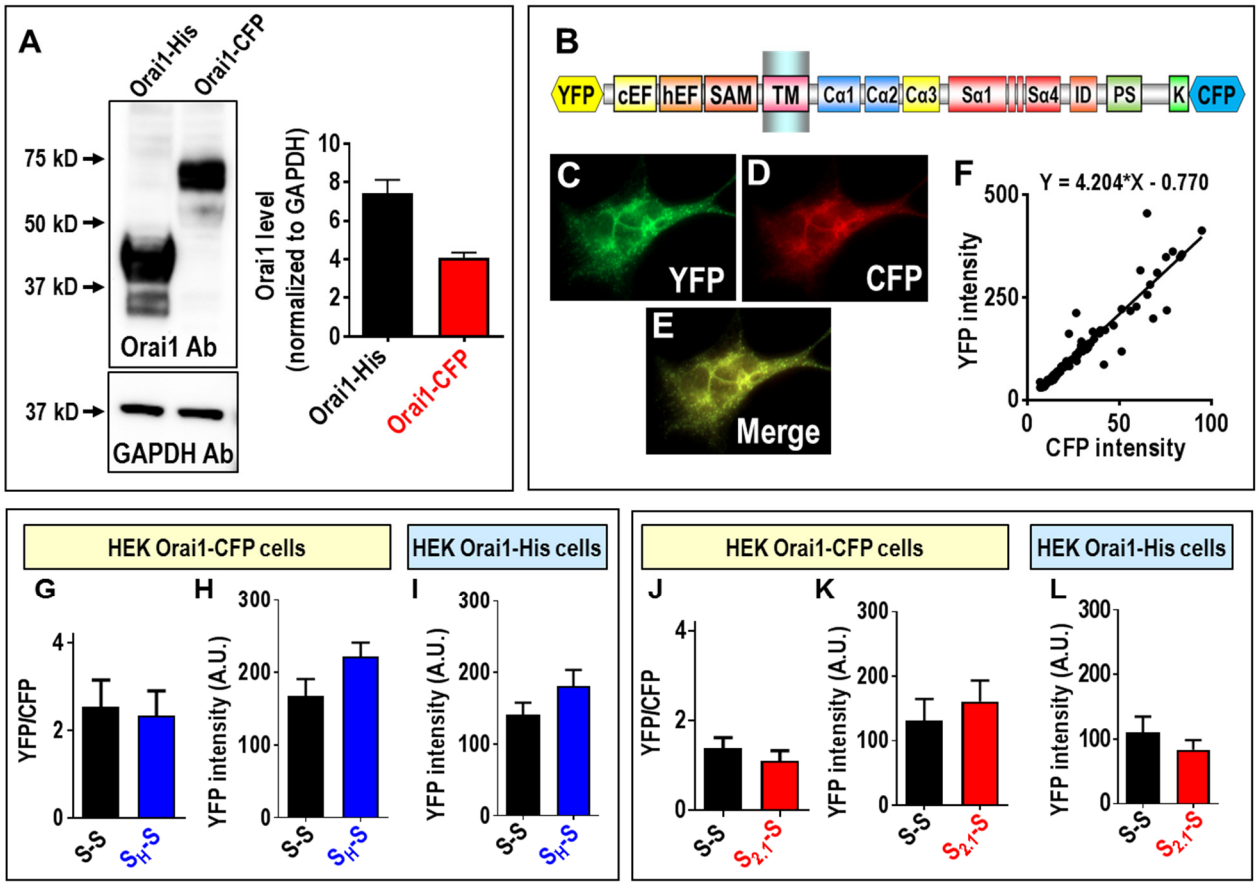

Fig. S4. Calibration of Orai1 channel expression to quantitate SOAR1 dimer-induced current activation. In order to relate the current density to the actual expression of each YFP-SOAR dimer, it was important to ensure that Orai1-His was expressed in excess over YFP-SOAR dimers. In this way, Orai1 current density would be dependent on how many functional SOAR units were present. (*A*) Since the Orai1-His protein is non-fluorescent, we needed to directly compare Orai1 protein expression in our stable HEK Orai1-His and stable HEK Orai1-CFP cell lines, by Western analysis. We quantified the relative expression of Orai1-His and Orai1-CFP using an Orai1 antibody, normalizing expression to GADPH. This showed that Orai1 expression in HEK Orai1-His cells was approximately two-fold higher than in Orai1-CFP cells. (*B-F*) In order to calibrate expression of YFP-SOAR1 dimers relative to Orai1-CFP channels, we designed a CFP-STIM1-YFP calibration construct to convert YFP/CFP fluorescence intensity ratio into molar ratio. (*B*) Diagram of the CFP-STIM1-YFP calibrator protein expressed in ER membrane, in which the CFP is restricted to the lumen of the ER and the YFP to the cytosol. Cells expressing this construct were treated with TG for 10 min to activate and unfold the STIM1 protein to maximize the distance between CFP and YFP. Subsequently, it was imaged for YFP, CFP and merged fluorescence *(C, D* and *E)*. *(F)* Fluorescence from calibrator protein images was quantified and plotted to calibrate YFP to CFP fluorescence under conditions in which the ratio of the two fluorescent molecules is known to be 1:1. The slope of this plot provided the fluorescence intensity ratio of YFP:CFP. Under our patch-clamp conditions, the intensity ratio was measured as 4.204. (*G*) Summary of the fluorescence intensity ratio of YFP/CFP for the data shown in Fig 2*J*. YFP-S-S (2.53 ± 0.62; n=15 cells), YFP-S_H-S (2.33 ± 0.57; n=14 cells). Based on the intensity ratio of YFP to CFP measured above (4.204), this shows that Orai1-CFP was almost 2-fold in excess of the YFP-SOAR dimers, thus, Orai1 was in excess for the patch clamp experiments. (*H*) Summary of the

YFP fluorescence intensity for YFP-S-S and YFP-S_H-S transiently transfected in HEK Orai1-CFP cells shown in Fig 2*J*. YFP-S-S (167.9 ± 23.2; n=15 cells), YFP-S_H-S (222.0 ± 19.0; n=14 cells). (*I*) Summary of the YFP fluorescence intensity for YFP-S-S and YFP-S_H-S for the data collected from HEK Orai1-His cells shown in Fig 2*H*. We analyzed HEK Orai1-His cells with YFP intensity similar or smaller than that shown in Fig S4*H*. YFP-S-S (141.5 ± 16.5; n = 12 cells), YFP-S_H-S (181.2 ± 22.5; n = 15 cells). Since Orai1-His expression is higher than Orai1-CFP, this ensured the Orai1-His was in excess over SOAR dimers. *(J*) Summary of the fluorescence intensity ratio of YFP/CFP for the data shown in Fig 4*O*. YFP-S-S (1.39 ± 0.23; n=6 cells), YFP-$S_{2.1}$-S (1.10 ± 0.22; n=7 cells). The Orai1-CFP was almost 3-fold in excess of the YFP-SOAR dimers. (*K*) Summary of YFP fluorescence intensity for YFP-S-S and YFP-$S_{2.1}$-S transiently transfected in HEK Orai1-CFP cells shown in Fig. 4*O*. YFP-S-S (130.9 ± 33.6; n=6 cells), YFP-$S_{2.1}$-S (161.0 ± 32.3; n=7 cells). (*L*) Summary of YFP fluorescence intensity for YFP-S-S and YFP-$S_{2.1}$-S transiently transfected in HEK Orai1-His cells shown in Fig 4*Q*. To ensure that Orai1-His is in excess, we analyzed cells with YFP intensity similar to or smaller than that shown in Fig S4*K*. YFP-S-S (109.9 ± 24.0; n=15 cells), YFP-$S_{2.1}$-S (83.5 ± 14.8; n=6 cells). Western blots are representative of three independent experiments. All data are presented as means ± SEM.

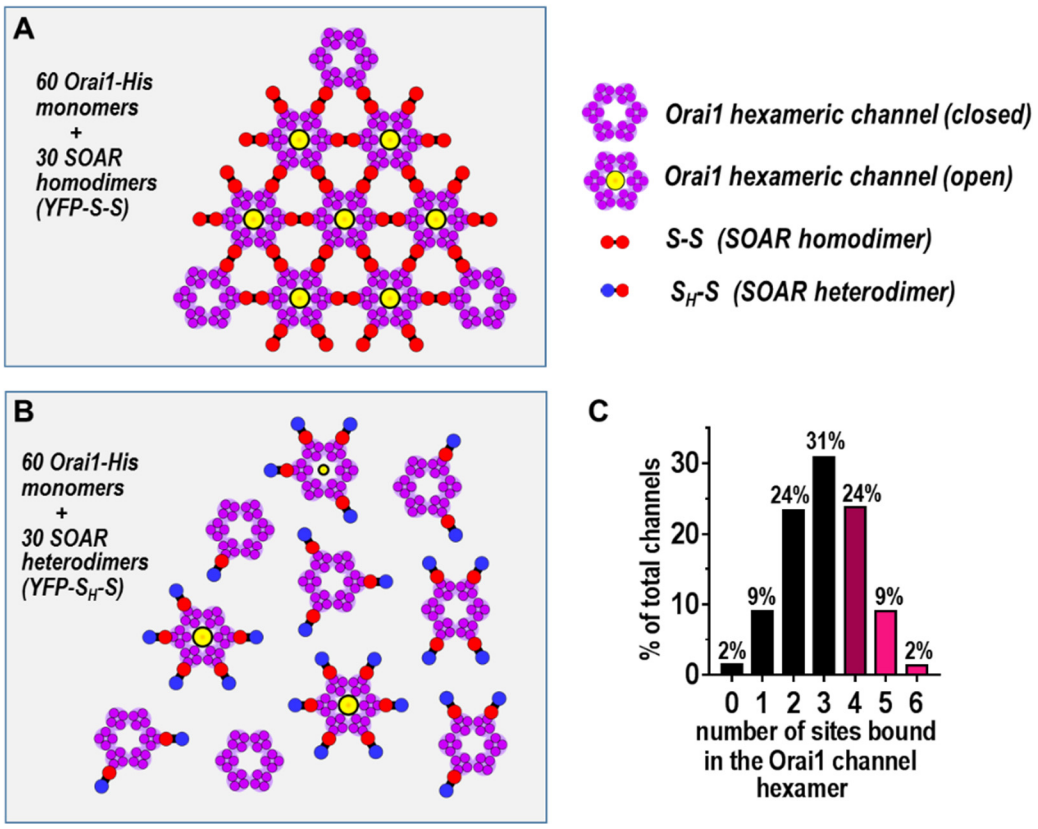

Fig. S5. Model of the possible coupling distribution of SOAR dimers with Orai1 channels. (*A*) Under conditions in which cross-linking is permitted (expression of Orai1-His with the YFP-S-S homodimer), the model shows the theoretical maximal channel activation that could occur with a ratio of Orai1 monomers to SOAR1 dimers of 2 to 1, similar to the ratio existing in the electrophysiology experiments shown in Fig. 2*G-J* (see Fig. S4*A-I*). In this case, there are 60 Orai1 monomer subunits (forming 10 channel hexamers) together with 30 SOAR1 wildtype homodimers. Theoretically, Orai channel cross-linking by SOAR dimers would permit up to 7 out of the 10 channels (70%) to be fully activated. In a large population of channels with the same 2:1 ratio expression, the theoretical percentage of active channels could approach 80%. (*B*) Under conditions in which cross-linking is not possible (expression of Orai1-His with the YFP-S_H-S heterodimer), with the same 2:1 ratio of expression (60 Orai1 monomer subunits with 30 SOAR1 heterodimers) we would assume that the active wildtype SOAR subunit in each YFP-S_H-S heterodimer would associate randomly with the Orai1 channels. In this case, few of the hexameric channels would have a full complement of 6 SOAR subunits attached. (*C*) In a large population of Orai1 channels expressed with the same 2:1 ratio of YFP-S_H-S heterodimer, the random association of SOAR heterodimers would theoretically result in the bell-shaped distribution of SOAR dimers bound to hexamers, as shown. Only 2% of Orai1 channels would have a full complement of six bound SOAR1 dimers, 9% would have five bound dimers, and 24% would have four bound dimers (Fig. S5*C*). While 6 SOAR units bound to an Orai1 hexamer would result in a fully active channel, we estimate that a channel with only 5 bound subunits might be 50% active, and a channel with only 4 subunits might be 25% active; 3 or less subunits bound results in no channel activity (2, 8). Therefore, theoretically, we might expect a total Orai1 activity of only 12.5% of full channel activity (2x100 + 9x50% + 24x25%). However, the observed current activity for YFP-S_H-S with Orai-His (43%) is substantially above this value. Similarly, the value for YFP-$S_{2.1}$-S with Orai1-His is also higher (35%), although in that case the Orai1-His to SOAR1 dimer expression ratio was 3:1 (see Fig. S4*L*). Likely, these results indicate that the SOAR dimer interaction with Orai1 channels is subject to significant positive cooperativity. Note that the expression of SOAR1 homodimers (YFP-S-S) or heterodimers (YFP-S_H-S) together with Orai1-CFP channels which do not permit channel cross-linking, would also be explained by the same logic given in (*B*) and (*C*).

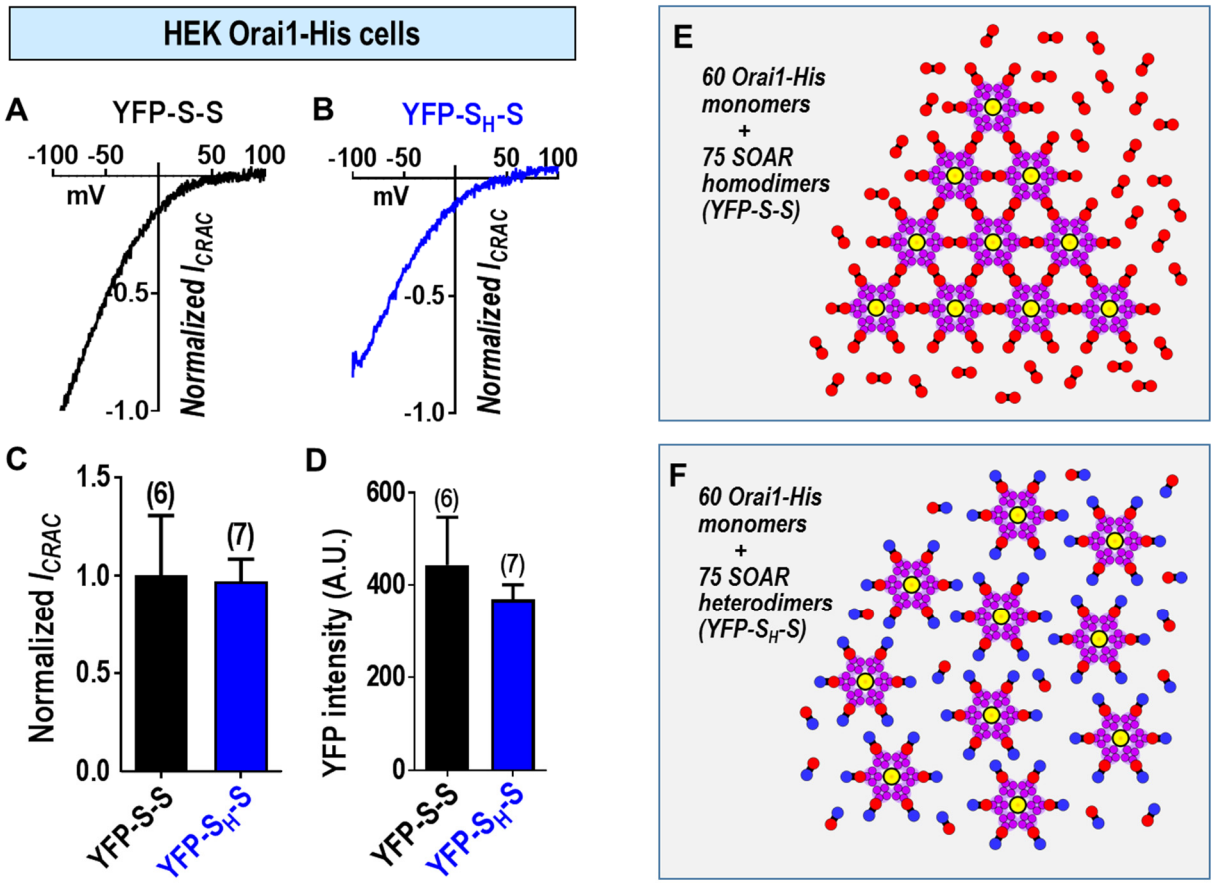

Fig. S6. Coupling distribution of Orai1-His channels and SOAR dimers measured under conditions of SOAR dimers in excess over Orai1-His channels. (*A*) Normalized I/V curve recorded in HEK Orai1-His cells expressing excess YFP-S-S. (*B*) Normalized I/V curve in HEK Orai1-His cells expressing excess YFP-S_H-S. (*C*) Summary of peak currents generated in HEK Orai-His cells by YFP-S-S and YFP-S_H-S. Current was normalized to YFP-intensity and expressed as a fraction of the mean current (normalized I_{CRAC}) measured with YFP-S-S in HEK Orai1-His cells. The value for YFP-S-S is 1.00 ± 0.31 (n=6 cells), and for YFP-S_H-S is 0.97 ± 0.11 (n=7 cells). (*D*) Summary of YFP fluorescence intensity for YFP-S-S and YFP-S_H-S transiently transfected in HEK Orai1-His cells; YFP-S-S (443.5 ± 103.1 AU; n=6 cells), YFP-$S_{2.1}$-S (368.9 ± 32.2 AU; n=7 cells). In Fig. S4I, the average YFP intensity of the YFP-SOAR homo/heterodimer was ~150 AU, giving an Orai1 to SOAR dimer ratio of 2:1. In the experiments shown in this figure, the average YFP intensity of YFP-S-S and YFP-SH-S) were ~400 AU, that is, 2.5 fold higher than that shown in Fig. 2H and Fig. S4I. Under this condition, the ratio of Orai1 to SOAR dimer was 1:1.25. For *A-D*, traces are representative of four independent experiments, and data are means ± SEM. (*E, F*) Coupling distribution of SOAR dimers and Orai channels under conditions in which the YFP-S-S or YFP-SH-S is in excess over Orai1 (Orai1-His:SOAR dimer ratio of 1:1.25), The diagram shows 60 Orai1-His monomer subunits (10 Orai1-His hexameric channels) coupling with 75 SOAR1 dimers or heterodimers. In this case, most Orai1-His channels are activated due to the excess of SOAR1 dimers, leading to the observation of similar whole cell currents for both YFP-S-S and YFP-SH-S.

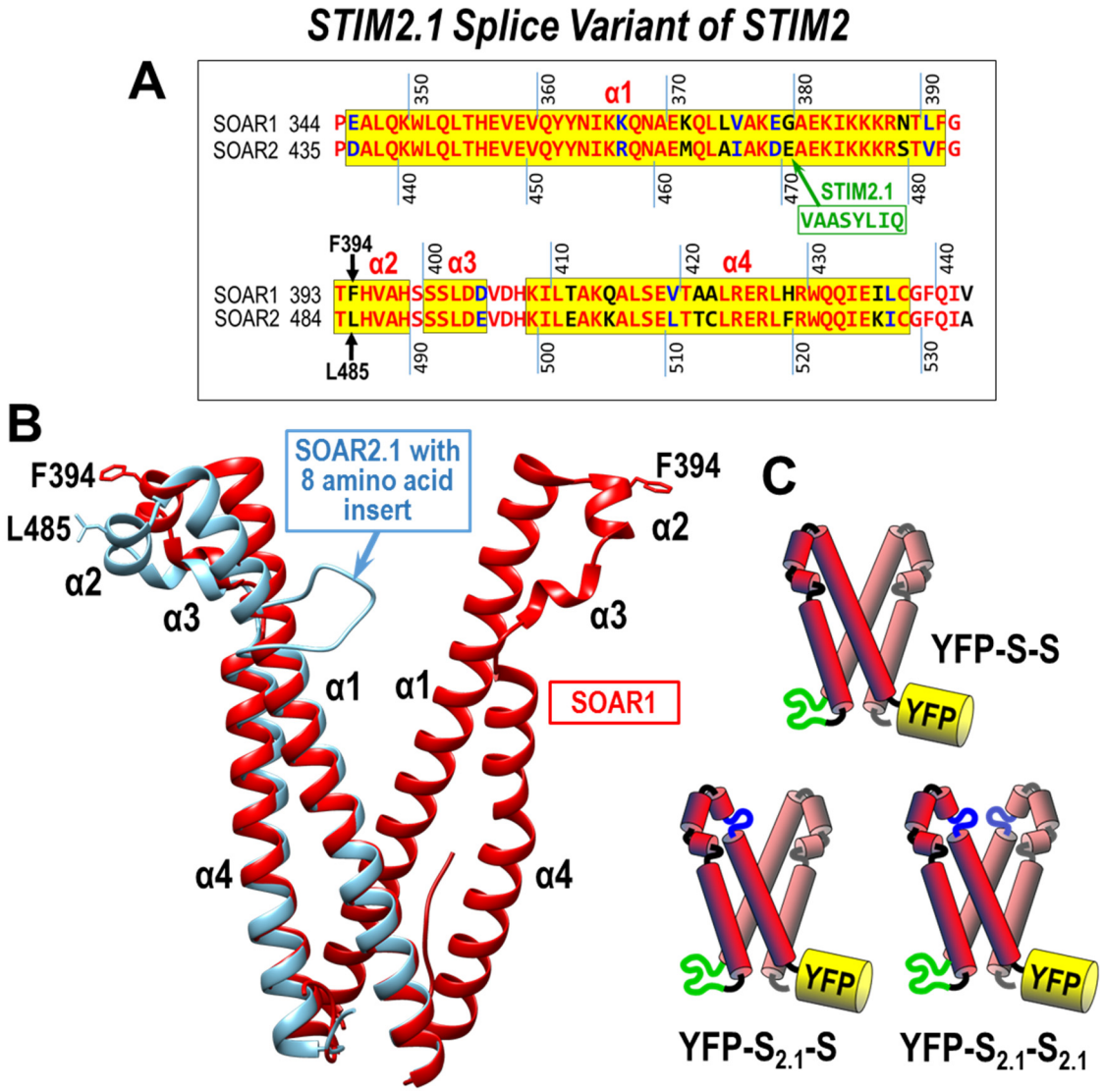

Fig. S7. Sequence and structure of the STIM2.1 splice variant. *(A)* Homology alignment of SOAR1 and SOAR2 reveals a strong sequence homology between the two proteins. The STIM2.1 splice variant contains an 8 amino acid insert derived from alternative splicing of the highly conserved exon 9 in STIM2 (9, 10). The 8 amino acid-insertion lies close to the critical Orai1-interacting site L485 residue (equivalent to F394 in SOAR1). *(B)* The SOAR1 dimer (red) is superimposed on a theoretical SOAR2.1-SOAR dimer (blue). Software based modeling indicates that the 8 amino acid insertion would significantly alter the structure of the α2 and α3 helices within the affected SOAR monomer, which is expected to significantly disrupt interactions with Orai1. *(C)* Schematic diagram of YFP-tagged SOAR2.1-containing dimers constructs: YFP-SOAR1-SOAR1 wildtype homodimer (YFP-S-S); YFP-SOAR2.1-SOAR1 heterodimer (YFP-$S_{2.1}$-S); YFP-SOAR2.1-SOAR2.1 mutant homodimer (YFP-$S_{2.1}$-$S_{2.1}$).

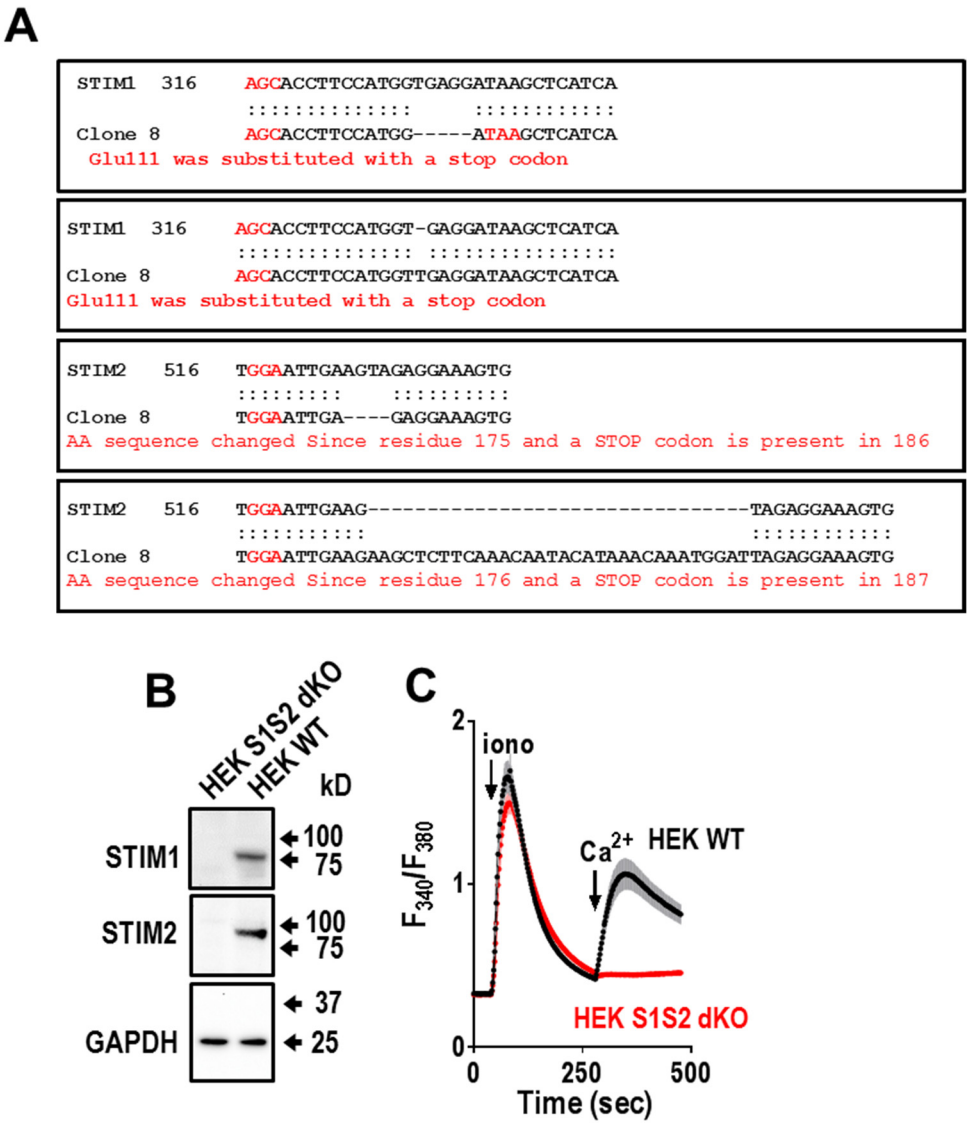

Fig. S8. Generation of the STIM1/STIM2 double knockout HEK cell line (HEK-S1S2-dKO). (*A*) Nucleotide sequencing reveals a frame shift mutation in clone 8 caused insertion of a stop codon to prematurely truncate STIM1 translation after Glu111. INDEL mutations in the STIM2 sequence introduced a stop codon at amino acid position 187, also causing premature truncation. (*B*) Western blot analysis confirmed that STIM1 and STIM2 expression were completely knocked out in clone 8. Comparison with HEK WT cells demonstrates that there are no detectible protein bands corresponding to STIM1 or STIM2 using antibodies specifically targeting each protein, respectively. (*C*) Ca^{2+} imaging reveals that store-operated Ca^{2+} entry was completely abolished in HEK-S1S2-dKO cells. Western blots and Ca^{2+} traces are representative of three independent experiments.

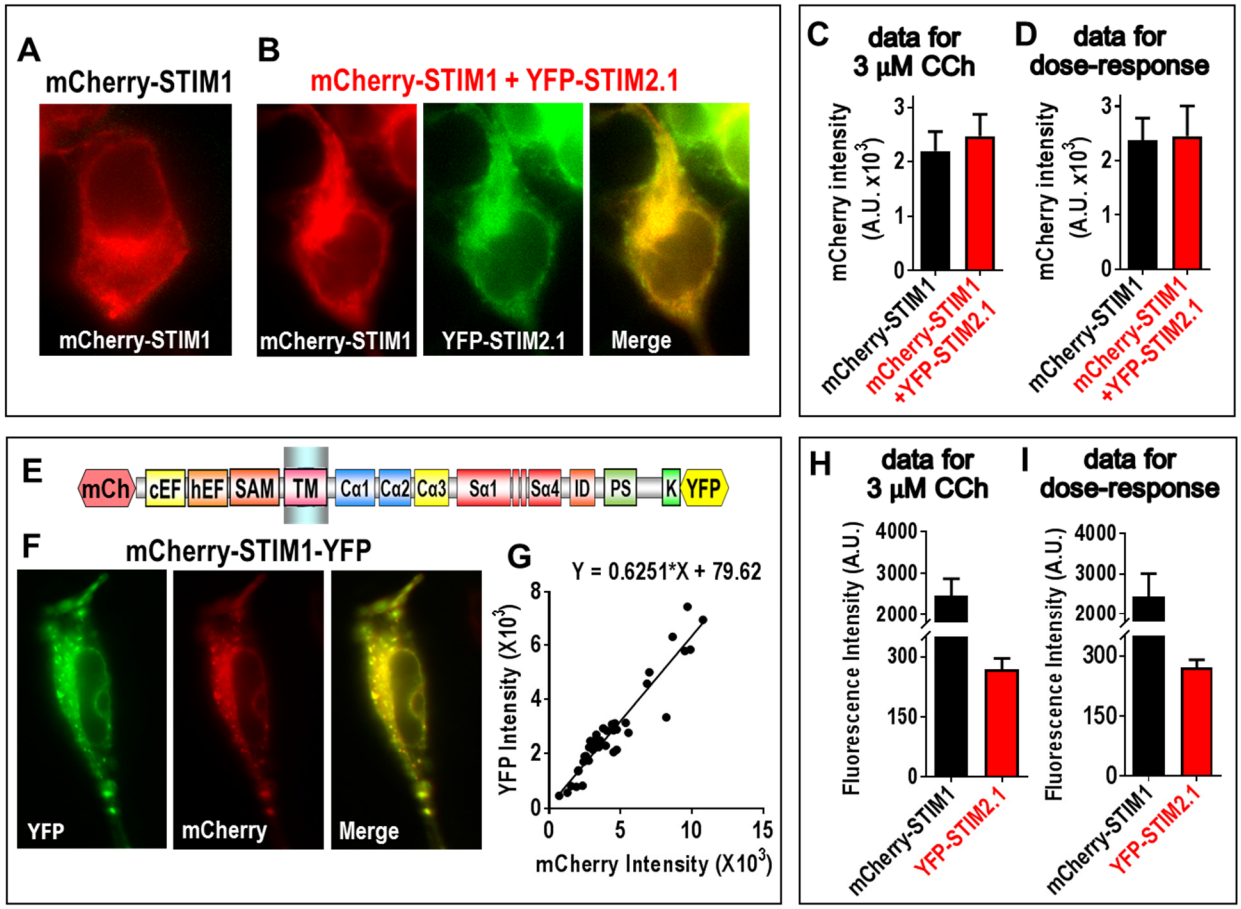

Fig. S9. Comparison and quantification of mCherry-STIM1 and YFP-STIM2.1 expression in HEK-S1S2-dKO cells for Fig. 5. (*A*) Fluorescence images of mCherry-STIM1 expressed in HEK-S1S2-dKO cells. (*B*) Images of co-expression of mCherry-STIM1 and YFP-STIM2.1 in HEK-S1S2-dKO cells. (*C*) Summary of mCherry-STIM1 fluorescence intensity for data shown in Fig. 5*A*-*C*, indicating similar level of STIM1 expression in the data shown in Fig. 5*A* and *B*. (*D*) Summary of mCherry fluorescence intensity for data shown in Fig. 5*D*-*G*, indicating similar expression level of STIM1 in Fig. 5*D* and *E*. (*E*-*G*) To calibrate expression of mCherry-STIM1 relative to YFP-STIM2.1, we designed the mCherry-STIM1-YFP calibration construct shown (*E*) to convert the YFP:mCherry fluorescence intensity ratio to the molar ratio for the experiments shown in Fig. 5*B* and *E*. Fluorescence images for YFP and mCherry of the calibration construct are shown in (*F*). In this experiment, the intensity ratio was 0.6251:1 when the molar ratio of YFP:mCherry was 1:1 (*G*). (*H*) Summary of the fluorescence intensity for the mCherry-STIM1 and YFP-STIM2.1 fluorescence data shown in Fig. 5*B*, giving a YFP:mCherry intensity ratio of 0.1091 and molar ratio for STIM2.1:STIM1 of approximately 1:5. (*I*) Summary of the fluorescence intensity for the mCherry-STIM1 and YFP-STIM2.1 fluorescence data shown in Fig. 5*E*, giving a YFP:mCherry intensity ratio of 0.1105 and molar ratio for STIM2.1:STIM1 of approximately 1:5. Images are representative of three independent experiments. Data are means ± SEM.

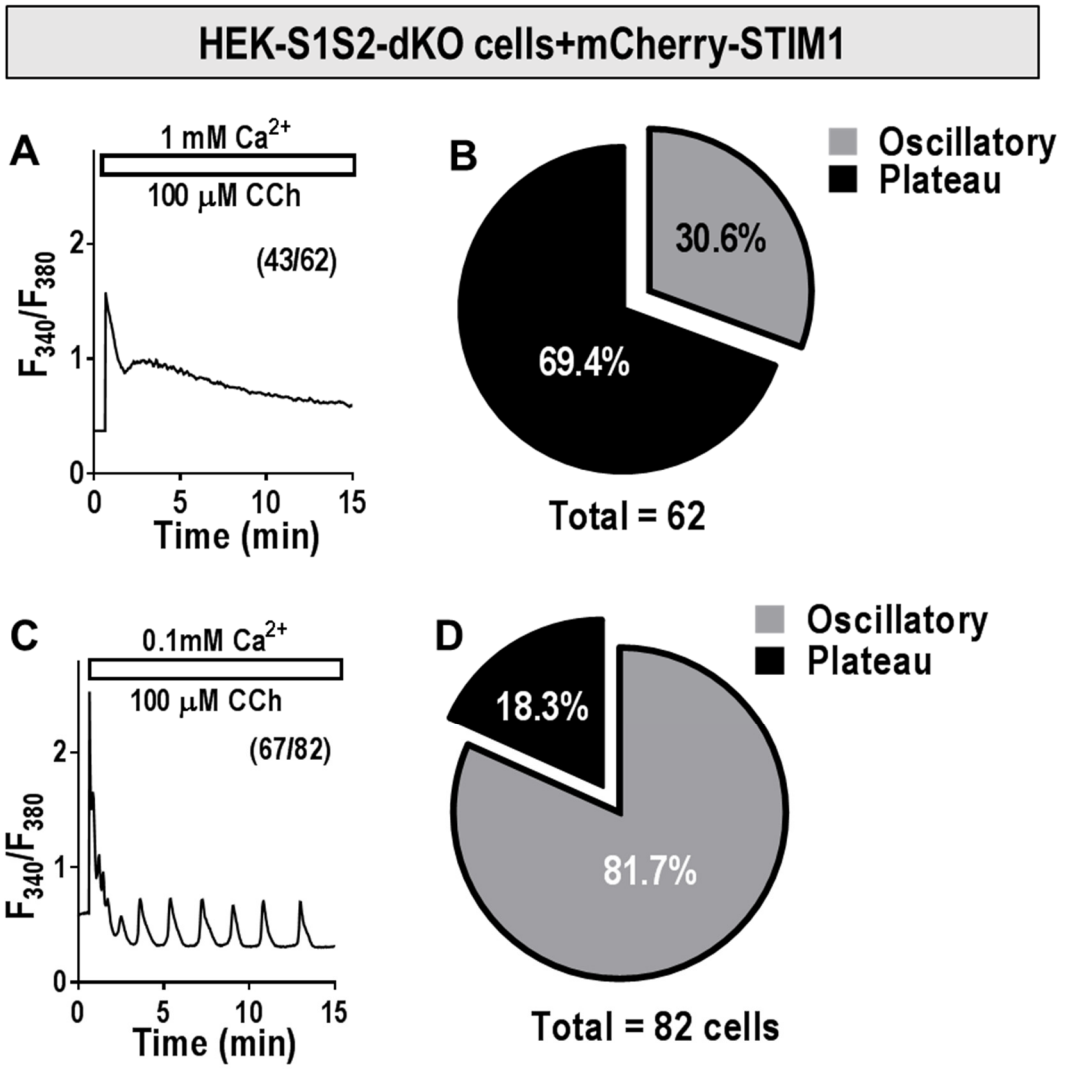

Fig. S10. Extracellular Ca^{2+} modifies the cytosolic Ca^{2+} response to CCh in HEK-S1S2-dKO cells transiently expressing mCherry-STIM1. (*A*) Representative Ca^{2+} trace in fura-2-loaded cells in 1 mM external Ca^{2+} solution in response to 100 μM CCh addition. (*B*) Chart showing that the majority of cells (69.4%; 43/62 cells) in (A) had plateau responses to 100 μM CCh, without oscillations. (*C*) Representative Ca^{2+} response to 100 μM CCh in fura-2-loaded cells with 0.1 mM extracellular Ca^{2+}. (*D*) Chart revealing that most cells in (*C*) displayed oscillatory Ca^{2+} responses to CCh stimulation (81.7%; 67 out of 82 cells). Data in (B) and (D) are the summary of all cells in three independent experiments.

References

1. Zhou Y, Wang X, Wang X, Loktionova NA, Cai X, Nwokonko RM, Vrana E, Wang Y, Rothberg BS, & Gill DL (2015) STIM1 dimers undergo unimolecular coupling to activate Orai1 channels. *Nat Commun* 6:8395.
2. Cai X, Zhou Y, Nwokonko RM, Loktionova NA, Wang X, Xin P, Trebak M, Wang Y, & Gill DL (2016) The Orai1 store-operated calcium channel functions as a hexamer. *J. Biol. Chem.* 291(50):25764-25775.
3. Zhou Y, Cai X, Loktionova NA, Wang X, Nwokonko RM, Wang X, Wang Y, Rothberg BS, Trebak M, & Gill DL (2016) The STIM1-binding site nexus remotely controls Orai1 channel gating. *Nat Commun* 7:13725.
4. Zal T & Gascoigne NR (2004) Photobleaching-corrected FRET efficiency imaging of live cells. *Biophys. J.* 86(6):3923-3939.
5. Kang M, Day CA, Kenworthy AK, & DiBenedetto E (2012) Simplified equation to extract diffusion coefficients from confocal FRAP data. *Traffic* 13(12):1589-1600.
6. Pettersen EF, Goddard TD, Huang CC, Couch GS, Greenblatt DM, Meng EC, & Ferrin TE (2004) UCSF Chimera - a visualization system for exploratory research and analysis. *J. Comput. Chem.* 25(13):1605-1612.
7. Yang X, Jin H, Cai X, Li S, & Shen Y (2012) Structural and mechanistic insights into the activation of Stromal interaction molecule 1 (STIM1). *Proc. Natl. Acad. Sci. U. S. A.* 109(15):5657-5662.
8. Yen M, Lokteva LA, & Lewis RS (2016) Functional Analysis of Orai1 Concatemers Supports a Hexameric Stoichiometry for the CRAC Channel. *Biophys. J.* 111(9):1897-1907.
9. Miederer AM, Alansary D, Schwar G, Lee PH, Jung M, Helms V, & Niemeyer BA (2015) A STIM2 splice variant negatively regulates store-operated calcium entry. *Nat Commun* 6:6899.
10. Rana A, Yen M, Sadaghiani AM, Malmersjo S, Park CY, Dolmetsch RE, & Lewis RS (2015) Alternative splicing converts STIM2 from an activator to an inhibitor of store-operated calcium channels. *J. Cell Biol.* 209(5):653-670.